

A new representation for non-local operators and path integrals

Paolo Amore*

*Facultad de Ciencias, Universidad de Colima,
Bernal Díaz del Castillo 340, Colima, Colima, Mexico*

(Dated: May 26, 2019)

We derive an alternative representation for the relativistic non-local kinetic energy operator and we apply it to solve the relativistic Salpeter equation using the variational sinc collocation method. Our representation is *analytical* and does not depend on an expansion in terms of local operators. We have used the relativistic harmonic oscillator problem to test our formula and we have found that arbitrarily precise results are obtained, simply increasing the number of grid points. More difficult problems have also been considered, observing in all cases the convergence of the numerical results. Using these results we have also derived a new representation for the quantum mechanical Green's function and for the corresponding path integral. We have tested this representation for a free particle in a box, recovering the exact result after taking the proper limits, and we have also found that the application of the Feynman-Kac formula to our Green's function yields the correct ground state energy. Our path integral representation allows to treat hamiltonians containing non-local operators and it could provide to the community a new tool to deal with such class of problems.

PACS numbers: 03.65.Ge, 02.70.Jn, 11.15.Tk

I. INTRODUCTION

The appearance of non-local operators in the relativistic extensions of the Schrödinger equation poses a serious challenge both to analytical and numerical calculations. However, the inclusion of relativistic effects is crucial for example in the study of meson phenomenology, where the Bethe-Salpeter equation (BSE) provides the correct theoretical tool to describe relativistic bound states. Replacing the kernel in the BSE with an instantaneous local potential one obtains a relativistic Schrödinger equation, which is also known as “spinless Salpeter equation” (SSE). In such case the hamiltonian operator is typically given by

$$\hat{H} = \sqrt{\hat{p}^2 + m^2} + V(\vec{r}) . \quad (1)$$

From a technical point of view, the inclusion in the Hamiltonian of the relativistic kinetic energy operator, $\sqrt{\hat{p}^2 + m^2}$, complicates the solution of the problem because of its non-local nature. The great phenomenological relevance of the SSE has motivated in the past twenty years many efforts to solve this equation, either using analytical or numerical techniques. Early work on this subject is contained for example in [1, 2, 3, 4, 5]. The method described in [4], which allows one to obtain a matrix representation of the non-local kinetic energy operator, has also been used recently [13] in conjunction with the Lagrange mesh method. In this case, the method is particularly appealing since it does not require the evaluation of the matrix elements of the potential, but rather only the specification of the potential on the grid points. This feature is also shared by the so called sinc collocation methods (see for example [6, 7]), which could also be used straightforwardly together with the method of [4]: however we do not consider this possibility since we are rather interested in developing a completely new approach, as it will soon become clear.

In a series of recent works, Lucha and collaborators have been able to obtain precise upper and lower bounds to the eigenvalues of the RSE, [8, 9, 10, 11]: these bounds provide useful analytic or semi-analytic expressions and have been applied to a number of test problems (see for example [11]). Another approach has been followed in [12], where an effective hamiltonian of non-relativistic form, which includes relativistic effects by means of parameters depending on the momentum, was constructed.

Finally, in a recent paper by Zhi-Feng and collaborators, [14], the SSE was studied in the case of the relativistic harmonic oscillator (RHO): in this case the authors were able to obtain recurrence relations for the coefficients of the series defining the eigenfunctions. The reader can also find useful the detailed bibliographic information contained in that paper.

*Electronic address: paolo@ucol.mx

The main purpose of the present paper is to develop a completely new approach to the solution of the SSE: we will derive an *analytical* representation of the non-local kinetic energy operator and use it with the Variational Sinc collocation Method (VSCM) [6] to obtain arbitrarily precise numerical results. We will use the RHO of [11], for which semi-analytical results are available, to test our approach. The new representation that we have found for the relativistic kinetic energy operator has also been generalized to the calculation of the quantum mechanical Green's function and has allowed us to obtain a new formula, which differs from the standard formula of path integrals.

The paper is organized as follows: in Section II we describe the SSE for the RHO and obtain precise numerical solutions working in momentum space configuration (these results are then compared with the results of [14]); in Section III we obtain an explicit analytical expression for the matrix elements of the non-local kinetic energy operator in terms of the so called “little sinc function” (LSF) recently introduced in [7]; we use this representation in the VSCM working in coordinate space and reproduce the results previously obtained in momentum space; in Section IV we extend our method to obtain explicit analytical representation for the Green's function which holds for general potentials; finally in Section V we draw our conclusions and set the direction for future work.

II. THE RELATIVISTIC HARMONIC OSCILLATOR

The RHO problem corresponds to the case in which a spherical harmonic oscillator potential, $V(\vec{r}) = ar^2$, is used in the Hamiltonian of eq. (1). After a simple rescaling of the mass and of the energy the Schrödinger equation can be cast in the form

$$\left[\sqrt{\hat{p}^2 + \mu^2} + r^2 \right] |\psi\rangle = \varepsilon |\psi\rangle, \quad (2)$$

depending on a single parameter μ ¹. The advantage of considering this potential lies in the fact that the corresponding Schrödinger equation in momentum space representation is local and it can therefore be attacked with standard techniques. In this case we are left with the equation

$$\left[-\Delta_p + \sqrt{p^2 + \mu^2} \right] \Psi(p) = \varepsilon \Psi(p), \quad (3)$$

where $\Delta_p \equiv \frac{\partial^2}{\partial p_x^2} + \frac{\partial^2}{\partial p_y^2} + \frac{\partial^2}{\partial p_z^2}$.

The authors of [14] focus their analysis on the $l = 0$ solutions and obtain a recurrence relation for the coefficients of the reduced radial wave function $y(p) = \sqrt{4\pi} p \Psi(p)$.

We will use the VSCM of [6, 7] to obtain a numerical solution of the problem and then compare our solution with the results of [14]. The VSCM uses sinc functions (SF), defined on the real line, or “little sinc functions” (LSF)[7], a particular generalization of sinc functions defined on finite intervals, to solve the Schrödinger equation by a collocation technique. Since the details of this method are clearly explained in [6, 7], we will here avoid mentioning all the technical details focusing on giving a more qualitative picture.

SF and LSF are functions which are strongly peaked around a certain value and they fastly decay and oscillate, when moving away from this value. Under certain conditions they can be chosen to be orthogonal: such set of orthogonal functions is obtained by performing a replica of one function at the points where this function vanishes, thus effectively introducing a grid. Unless otherwise specified, either by the Physics of the problem or by convention, the spacing of the grid is *arbitrary* and, if not carefully chosen, it strongly affects the precision of the results. In a recent paper Amore et al. have used an arbitrary scale factor as a variational parameter in the solution of the Schrödinger equation using a basis of simple harmonic oscillator wave functions [15]: in that case it was shown that the optimal scale factor could be chosen to minimize the trace of the Hamiltonian matrix in the Hilbert subspace spanned by the N elements of the basis. The same principle, which was inspired by the Principle of Minimal Sensitivity (PMS) [16], was then used in [6, 7] using a sinc collocation technique. As mentioned in the Introduction the sinc collocation has the great advantage of avoiding the evaluation of matrix elements of the potential, which is simply “collocated” at the grid points; on the other hand the evaluation of the matrix elements of the non-relativistic kinetic operator is also quite simple, since it involves matrices whose elements are obtained by collocating the derivative of a given sinc function at the grid points. In this way one easily obtains a matrix representation for the Hamiltonian.

For example in one dimension one has

$$H_{kl} = -\frac{\hbar^2}{2m} c_{kl}^{(2)} + \delta_{kl} V(kh). \quad (4)$$

¹ We adopt the same notation used in [14].

TABLE I: $\varepsilon - \mu$ for different numbers of grid points using $\mu = 30$. P_{PMS} is the optimal region where LSF are defined, obtained using the PMS.

N	P_{PMS}	$\varepsilon - \mu$
10	11.117	0.386276142683809727673228675763
20	15.871	0.386266042582133375751633823806
30	19.611	0.386266042572445208567680793779
40	22.835	0.386266042572445193517230825356
50	25.735	0.386266042572445193517188444455
exact		0.386266042572445193517188444455

where $c^{(2)}$ is the matrix obtained from the second derivative of the sinc functions. h is the grid spacing. In the following we will set $\hbar = 1$, so that h will not be confused with the Planck constant.

The diagonalization of H allows one to obtain the eigenvalues (energies) and the eigenvectors (wave functions) of the problem (the number of these eigenvalues and eigenvectors being equal to the number of sinc functions used).

Before trying to deal with the RHO in coordinate space, where it is non-local, we wish to use the VSCM to find numerical solutions in momentum space, where it is local. In this case machinery of VSCM applies straightforwardly and we are able to verify our claim of accuracy of our method. To allow a comparison with [14] we use $\mu = 30$.

In Table I we display the values of $\varepsilon - \mu$ for $\mu = 30$ using grids with different N . P_{PMS} is the width of the region in momentum space where the RHO is solved and it is obtained using the PMS. Our results show that the method converges quite rapidly (for $N = 50$ all the 30 digits are already correct). A direct comparison with Table 1 of [14] shows complete agreement, although the results of [14] contain only 6 digits.

However we can also perform a more accurate test using the recurrence relations for the coefficients appearing in the series for the wave functions given in [14]. In fact, we can easily extract these coefficients by expanding around $p = 0$ the wave function obtained with our method and then we can compare them with the results obtained using directly the recurrence relation of eq.(8) of [14]. To avoid conflicts with our notation we call these coefficients \bar{c}_n (c_n in [14]). In Fig.1 we have plotted the relative error $\Xi \equiv (\bar{c}_n^{(rec)} - \bar{c}_n^{(num)})/\bar{c}_n^{(rec)} \times 100$, where $\bar{c}_n^{(rec)}$ and $\bar{c}_n^{(num)}$ are obtained from the recurrence relations (using the numerical value obtained for ε with our method) and from our calculated wave function, expanded around $p = 0$, respectively. The plot confirms that our method converges strongly and that our results are in perfect agreement with the semi-analytical formulas of [14]. $N - 1$ specified in the plot is the number of sinc functions used.

The importance of the RHO lies in the unique possibility of having a complete control on the solutions of the problem, which can be calculated to any desired accuracy, despite retaining the non-local nature of the kinetic energy operator. In more general problems, when the potential is not quadratic in the coordinates, one cannot recover a local Schrödinger equation by working in the momentum space configuration. In these cases one possibility is to resort to a non-relativistic expansion in powers of p/μ , which to lowest order provides the rest mass and the usual non-relativistic kinetic energy:

$$\sqrt{p^2 + \mu^2} \approx \mu + \frac{p^2}{2\mu} + \dots \quad (5)$$

However the hamiltonian operator obtained in this way contains derivatives of higher order. In such cases it is still possible to apply the VSCM in coordinate space to solve these equations, by using the matrices corresponding to the higher order derivatives (which can be computed quite easily). Although the implementation of this procedure poses no problem, we wish to show that in certain cases it can provide unexpected results, such as results which converge to wrong solutions as the higher order relativistic corrections are added.

We use once again the RHO as our “guinea pig” and work in momentum space configuration using a potential obtained by expanding the kinetic term up to a give order in p^2/μ^2 . The expression in eq. (5), for example, would represent the potential obtained working to order p^2/μ^2 and corresponds to the usual non-relativistic harmonic oscillator. However, in the inclusion of the higher order terms we have to take into account that terms of order $(p^2/\mu^2)^{2n}$, with n integer, are negative, and therefore one always needs to work to order $(p^2/\mu^2)^{2n+1}$ to have a spectrum bounded from below. We call $\tilde{V}_{2n+1}(p)$ the potential in momentum space corresponding to the expansion

TABLE II: $\varepsilon - \mu$ using $N = 100$ and $\mu = 30$ and the local potentials $V_n(p)$.

$2n + 1$	$\varepsilon - \mu$ for $\mu = 30$	$\varepsilon - \mu$ for $\mu = 5$
1	0.387298334620741688517926539978	0.94868329805051379959966806333
3	0.386266420436379405327465768718	0.917998080358892779439199865797
5	0.386266043099402218130055135176	0.916146523799889657008305183814
7	0.386266042574045836353234202429	0.915846448935051044197245795013
9	0.386266042572453671527365247948	0.91581315161430089514610659534
11	0.386266042572445262852791751103	0.915869030516899002389616443215
13	0.38626604257244519432768972826	0.915969994254155249594896088725
15	0.38626604257244519353002484604	0.916099070146014646820188963944
17	0.386266042572445193517453256126	0.916247177257518912927253345858
19	0.38626604257244519351719534876	0.916408388764026715314316265532
21	0.38626604257244519351718866641	0.916578441604180056427277884484
23	0.386266042572445193517188452906	0.916754138752643598204761050323
25	0.386266042572445193517188444656	0.916933043994378840230769667954
27	0.386266042572445193517188444277	0.917113292696937291931397089421
29	0.386266042572445193517188444256	0.9172934594683484794299701287
31	0.386266042572445193517188444255	0.917472459781309119739340192984
exact	0.386266042572445193517188444255	0.915319412084543926332745726574

to order $(p^2/\mu^2)^{2n+1}$. For example to order $(p^2/\mu^2)^3$ we have

$$\tilde{V}_3(p) = \mu + \frac{p^2}{2\mu} - \frac{p^4}{8\mu^3} + \frac{p^6}{16\mu^5}. \quad (6)$$

Once we substitute the non-local operator with its local expansion to a given odd order we can solve the corresponding local Schrödinger equation and thus obtain the energies and the wave functions. In the second column of Table II we report the values of $\varepsilon - \mu$ for the ground state of the potential using $N = 100$ and $\mu = 30$ and $\mu = 5$ respectively. While the series for $\mu = 30$ converges to the exact result within 30 digit precision for \tilde{V}_{31} , for $\mu = 5$ it is clear that the series does not converge to the exact result, providing its best approximation for \tilde{V}_9 .

We can give a simple explication of this behavior: for $p > \mu$ the series in eq. (5) – where p is now a real number – diverges and therefore the potential obtained using this series, $\tilde{V}_\infty(p) = \lim_{n \rightarrow \infty} \tilde{V}_{2n+1}(p)$, corresponds to the original potential with an infinite wall located at $p = \mu$. In the case $\mu = 30$ the wave function is extremely small at $p = \mu$ (dashed line in the left plot of Fig. 2) and therefore the non-relativistic expansion is capable of providing highly (but not arbitrarily) accurate results (see Table II); on the other hand, in the case $\mu = 5$ (solid line in the left plot of Fig. 2) the wave function is sizeable at $p = \mu$ and the non-relativistic expansion provides a very poor approximation (see the third column of Table II). The situation would clearly get worse as μ is taken to be smaller.

It should be stressed that in both cases the non-relativistic expansion does converge, although not to the exact result, but rather to a value which depends on the scale μ . I am not aware if this is a well-known fact in the literature. In the case $\mu = 5$, the limit which the results of Table II tend to is $[\varepsilon - \mu]_\infty = 0.929172020669205909804169248218$.

III. MATRIX ELEMENTS OF $\sqrt{\hat{p}^2 + \mu^2}$

In this Section we want to describe a new way of calculating the matrix elements of the relativistic kinetic energy operator, which avoids the problems of the local non-relativistic expansion described in the previous Section.

As mentioned in the Introduction, there are approaches in the literature to calculate the matrix elements of this operator, although they are numerical. For example, the method described in [4] consists of 4 steps, i.e. the computation of $(M^2)_{ij} = \langle i | \hat{p}^2 + \mu^2 | j \rangle$, the diagonalization of M^2 , the computation of the diagonal square root matrix and finally the computation of the square root matrix M . Because of the calculation of M is numerical this procedure would not be profitable in a variational scheme, where the PMS condition is always analytical.

However, we will now show that it is possible to obtain *once and for all* an analytical representation of $\sqrt{\hat{p}^2 + \mu^2}$ and indeed of any non-local operator which is function of the momentum operator. Because our results will be analytical it will be possible to extend the VSCM to include relativistic non-local terms, in what we will call “Relativistic variational collocation method” (RVSCM).

Let us now present our results. We will work in the following with the Little Sinc Functions (LSF) of [7], although similar results can also be obtained with the usual sinc functions². The LSF have been obtained in [7] using the orthonormal basis of the wave functions of a particle in a box with infinite walls located at $x = \pm L$:

$$\psi_n(x) = \frac{1}{\sqrt{L}} \sin\left(\frac{n\pi}{2L}(x+L)\right). \quad (7)$$

A LSF is simply obtained as

$$s_k(h, N, x) = \frac{2L}{N} \sum_{n=1}^N \psi_n(x) \psi_n(y_k), \quad (8)$$

where $y_k \equiv \frac{2kL}{N} = kh$. The LSF should be regarded as an approximate representation of a Dirac delta function. To simplify the notation we have introduced the grid spacing $h \equiv 2L/N$. k is an integer which takes the values $k = -N/2 + 1, -N/2 + 2, \dots, N/2 - 1$, each corresponding to a different grid point.

As shown in [7] an explicit expression for the LSF can be obtained for even values of N in the form

$$s_k(h, N, x) = \frac{1}{2N} \left\{ \frac{\sin\left(\left(1 + \frac{1}{2N}\right) \frac{\pi}{h}(x - kh)\right)}{\sin\left(\frac{\pi}{2Nh}(x - kh)\right)} - \frac{\cos\left(\left(1 + \frac{1}{2N}\right) \frac{\pi}{h}(x + kh)\right)}{\cos\left(\frac{\pi}{2Nh}(x + kh)\right)} \right\}. \quad (9)$$

After simple algebra one can also obtain the alternative expression

$$s_k(h, N, x) = -\frac{1}{N} \sum_{n=-N}^{+N} (i)^{n+1} \sin\left(\frac{n\pi}{2} + \frac{kn\pi}{N}\right) e^{i\frac{n\pi x}{2L}} \quad (10)$$

which is suited to calculate the action of $\sqrt{\hat{p}^2 + \mu^2}$ over a LSF:

$$\sqrt{\hat{p}^2 + \mu^2} s_k(h, N, x) = -\frac{1}{N} \sum_{n=-N}^{+N} (i)^{n+1} \sin\left(\frac{n\pi}{2} + \frac{kn\pi}{N}\right) \sqrt{\left(\frac{n\pi}{2L}\right)^2 + \mu^2} e^{i\frac{n\pi x}{2L}}. \quad (11)$$

Upon collocation on the grid, i.e. after setting $x \rightarrow x_j$, we have the matrix element

$$K_{kj} = \sqrt{\hat{p}^2 + \mu^2} s_k(h, N, x_j) = -\frac{1}{N} \sum_{n=-N}^{+N} (i)^{n+1} \sin\left(\frac{n\pi}{2} + \frac{kn\pi}{N}\right) \sqrt{\left(\frac{n\pi}{2L}\right)^2 + \mu^2} e^{i\frac{jn\pi}{N}}. \quad (12)$$

Notice that, despite its appearance, the expression above is real, as it would be evident expressing it in terms of trigonometric functions; however, we prefer to leave it in terms of plane waves.

To check that eq. (12) is indeed the correct matrix element of the non-local kinetic energy operator we can calculate the matrix product $(K^2)_{kl} = \sum_j K_{kj} K_{jl}$

$$\begin{aligned} (K^2)_{kl} &= \sum_j K_{kj} K_{jl} = \frac{1}{N^2} \sum_{j=-N/2+1}^{N/2-1} \sum_{n_1=-N}^{+N} \sum_{n_2=-N}^{+N} (i)^{n_1+n_2+2} \sin\left(\frac{n_1\pi}{2} + \frac{kn_1\pi}{N}\right) \sin\left(\frac{n_2\pi}{2} + \frac{jn_2\pi}{N}\right) \\ &\quad \sqrt{\left(\frac{n_1\pi}{2L}\right)^2 + \mu^2} \sqrt{\left(\frac{n_2\pi}{2L}\right)^2 + \mu^2} e^{i\frac{(jn_1+ln_2)\pi}{N}} \end{aligned} \quad (13)$$

² As a matter of fact it is shown in [7] that for $N \rightarrow \infty$ and keeping h fixed the LSFs reduce to the SFs.

TABLE III: $\varepsilon - \mu$ for different numbers of grid points using $\mu = 30$ and working in coordinate space. L_{PMS} is the optimal region where LSF are defined, obtained using the PMS.

N	L_{PMS}	$\varepsilon - \mu$
10	1.413	0.386276142683809727673228675763
20	1.980	0.386266042582133375751633823806
30	2.403	0.386266042572445208567680793779
40	2.752	0.386266042572445193517230825356
50	3.052	0.386266042572445193517188444455
exact		0.386266042572445193517188444255

and compare it with the matrix $(K^2)_{kl} = (\hat{p}^2 + \mu^2)_{kl}$, calculated either using the very same eq. (12) with $\sqrt{\left(\frac{n\pi}{2L}\right)^2 + \mu^2} \rightarrow \left(\frac{n\pi}{2L}\right)^2 + \mu^2$ or using the matrix for the second derivative to represent \hat{p}^2 (see [7]).

We can define

$$\mathcal{C}_{n_1 n_2} \equiv \sum_{j=-N/2+1}^{N/2-1} e^{i \frac{j n_1 \pi}{N}} \sin\left(\frac{n_2 \pi}{2} + \frac{j n_2 \pi}{N}\right) \quad (14)$$

which for $n_2 = \pm n_1$ takes the values

$$\mathcal{C}_{n_1 n_1} = -\mathcal{C}_{n_1, -n_1} = -\frac{N}{2}(-i)^{n_1+1}. \quad (15)$$

When $\mathcal{C}_{n_1 n_2}$ is used inside eq. (13) it can be seen that only the terms corresponding to $n_2 = \pm n_1$ contribute, whereas the remaining terms cancel out. In this case we obtain

$$\begin{aligned} (K^2)_{kl} &= \frac{1}{N^2} \sum_{n_1=-N}^{+N} \sum_{n_2=-N}^{+N} (i)^{n_1+n_2+2} \sin\left(\frac{n_1 \pi}{2} + \frac{k n_1 \pi}{N}\right) \sqrt{\left(\frac{n_1 \pi}{2L}\right)^2 + \mu^2} \sqrt{\left(\frac{n_2 \pi}{2L}\right)^2 + \mu^2} e^{i \frac{l n_2 \pi}{N}} \\ &\quad \left(-\frac{N}{2}(-i)^{n_1+1}\right) (\delta_{n_1, n_2} - \delta_{n_1, -n_2}) \\ &= -\frac{1}{N} \sum_{n=-N}^{+N} (i)^{n+1} \sin\left(\frac{n \pi}{2} + \frac{k n \pi}{N}\right) \left[\left(\frac{n \pi}{2L}\right)^2 + \mu^2\right] e^{i \frac{l n \pi}{N}}. \end{aligned} \quad (16)$$

This completes our proof, since we have precisely obtained the expression that we would have reached if we had used eq. (12) directly with the squared operator. We have also verified numerically this result and confirmed its validity.

As done for the non-relativistic Schrödinger equation we can obtain the Hamiltonian matrix

$$H_{kl} = K_{kl} + \delta_{kl} V(kh), \quad (17)$$

which upon diagonalization provides a set of eigenvalues (energies) and eigenvectors (wave functions).

In Table III we have applied eq. (17) to the RHO with $\mu = 30$, i.e. the case considered in [14] and also studied in Tables I and II. The reader should appreciate that *the rate of convergence of the results of Table III is the same as the one of the results of Table I, although now we are working in configuration space with the non-local operator.* In Table IV we have also studied the RHO with $\mu = 5$, for which in the previous Section it was shown that the non-relativistic expansion would not converge to the exact result. In this case we see that the results converge to the exact result and for $N = 100$ all the displayed digits are correct (we notice a curious acceleration in convergence when going from $N = 90$ to $N = 100$). In the right plot of Fig.2 we show the wave functions for the RHO corresponding to $\mu = 5$ and to $\mu = 30$ in coordinate space³.

³ Notice that the wave functions in these plots are normalized to 1, whereas the wave functions displayed in Fig.1 of [14] are normalized to have a unit slope at the origin.

TABLE IV: $\varepsilon - \mu$ for different numbers of grid points using $\mu = 5$ and working in coordinate space. L_{PMS} is the optimal region where LSF are defined, obtained using the PMS.

N	L_{PMS}	$\varepsilon - \mu$
10	2.04	0.915501305135409803480675579464
20	2.691	0.91531962596043582355049899215
30	3.139	0.91531941362119216332139121675
40	3.491	0.915319412116470843532505890535
50	3.785	0.915319412085834123329714397391
60	4.041	0.915319412084625618689404973776
70	4.268	0.9153194120845510601444559315
80	4.473	0.91531941208454470855183044144
90	4.661	0.915319412084544017492153869561
100	4.836	0.915319412084543926332745726574
exact		0.915319412084543926332745726574

Although the results obtained studying the RHO are sufficient in our opinion to prove the efficiency and simplicity of the method that we are proposing in this paper, we wish to consider two examples which can better illustrate the power of our method.

As a first example we have chosen the potential

$$V(x) = \sqrt{a^2 + x^2} \quad (18)$$

and the corresponding SSE ($x \in (0, \infty)$):

$$\left[\sqrt{\hat{p}^2 + \mu^2} + \sqrt{a^2 + x^2} \right] \psi(x) = \varepsilon \psi(x) . \quad (19)$$

Notice that for $a \gg 1$ and $\mu \gg 1$ one recovers the standard harmonic oscillator (SHO). In Table V we show the numerical results for $\varepsilon - \mu$ (we consider the ground state) as a function of the number of grid points and assuming $a = \mu = 1$. The reader can appreciate the slower convergence of the results in this case.

As a second example that we wish to consider the SSE ($x \in (0, \infty)$):

$$\left[\sqrt{\hat{p}^4 + \hat{p}^2 + \mu^2} + \sqrt{a^2 + x^2} \right] \psi(x) = \varepsilon \psi(x) . \quad (20)$$

Although we do not have any physical model in mind when we write such equation, we are aware that modifications of the standard Schrödinger equation (not necessarily of this kind) appear in several areas of research: for example, the introduction of a minimal length uncertainty relation naturally leads to modified Schrödinger equations (see for example [17]). Table VI shows that the RVSCM for eq. (20), assuming $\mu = a = 1$, converges (for $N = 100$ there is a 11 digit accuracy). In Fig. 3 we have plotted the wave function for the ground state.

IV. GREEN'S FUNCTIONS

In this Section we want to show that the method that we have developed in the previous Section can also be applied to the calculation of matrix elements of other non-local operators. We will see that SF and LSF are a powerful tool, and actually they have already been used earlier in a different context in applications to Quantum Field Theory (QFT) (see for example [18]).

To start we consider an operator $\hat{O} \equiv f(\hat{p})$: in such case, the results that we have obtained in the previous Section apply straightforwardly and one obtains

$$O_{kj} = \frac{1}{N} \sum_{n=-N}^{+N} (i)^{n+1} \sin\left(\frac{n\pi}{2} + \frac{kn\pi}{N}\right) f\left(i\frac{n\pi}{2L}\right) e^{i\frac{jn\pi}{N}} . \quad (21)$$

TABLE V: $\varepsilon - \mu$ for different numbers of grid points using $\mu = 1$ and $a = 1$ with the potential of eq. (18) and working in coordinate space. L_{PMS} is the optimal region where LSF are defined, obtained using the PMS.

N	L_{PMS}	$\varepsilon - \mu$
10	3.963	2.07934094719878926096190043347
20	5.605	2.07592620109919594206959632052
30	6.865	2.07587363685392522399510596978
40	7.927	2.07587115531220883612932074407
50	8.862	2.07587095004525245939895643445
60	9.708	2.07587092616715904154251246677
70	10.49	2.07587092265838475425346729639
80	11.21	2.07587092204570010758927347719
90	11.89	2.07587092192338175659809635248
100	12.53	2.07587092189618183676133263454

TABLE VI: $\varepsilon - \mu$ for different numbers of grid points using $\mu = 1$ with the potential of eq. (20) and working in coordinate space. L_{PMS} is the optimal region where LSF are defined, obtained using the PMS.

N	L_{PMS}	$\varepsilon - \mu$
10	3.947	2.72104889005969931884957446171
20	5.597	2.72418061093820964822373363811
30	6.859	2.72420379685445988334890658856
40	7.923	2.72420013927494099660693661877
50	8.859	2.72419961847452319053688870223
60	9.705	2.72419958894693066253434331235
70	10.48	2.72419959587264127020051964698
80	11.21	2.72419959907480104025626097945
90	11.89	2.72419959986319344695865656933
100	12.53	2.72419959998345792641897335324

One example of application of this formula is the calculation of the Green's function for a free particle in a box, $|x| < L$, which is given by (see for example [19, 20])

$$G^{(0)}(y, 0; x, t) = \langle x | e^{-i\frac{p^2}{2\mu}t} | y \rangle .$$

The notation $|x\rangle$ indicates a state localized at a point x : in our formalism this is simply represented by a SF or a LSF with a peak at this point. Notice however that SF and LSF are not normalized to one, see [6, 7], which means that we have an extra factor $1/\sqrt{h} \equiv \sqrt{N/2L}$ for each SF or LSF, where h is the spacing of the grid.

Therefore we can write:

$$G^{(0)}(x_j, 0; x_k, t) = -\frac{1}{Nh} \sum_{n=-N}^{+N} (i)^{n+1} \sin\left(\frac{n\pi}{2} + \frac{kn\pi}{N}\right) e^{-it\left[\frac{1}{2\mu}\left(\frac{n\pi}{2L}\right)^2\right]} e^{i\frac{yn\pi}{N}} , \quad (22)$$

x_k and x_j being points on the grid. In the limit of an infinitely dense grid one can switch from the discrete indices k, j to the continuum indices x, y :

$$G^{(0)}(y, 0; x, t) = -\frac{1}{2L} \sum_{n=-N}^{+N} i^{n+1} e^{\frac{in\pi x}{2L} - \frac{in^2\pi^2 t}{8L^2\mu}} \sin\left(\frac{\pi y n}{2L} + \frac{\pi n}{2}\right) \quad (23)$$

Notice that in the case of a free particle the exact result can be calculated with the standard path integral and reads

$$G^{(0)}(0, 0; x, t) = \sqrt{\frac{\mu}{2\pi i t}} e^{i \frac{\mu x^2}{2t}}. \quad (24)$$

In our formalism we have

$$G^{(0)}(0, 0; x, t) = -\frac{1}{2L} \sum_{n=-N}^{+N} i^{n+1} e^{\frac{i n \pi x}{2L} - \frac{i n^2 \pi^2 t}{8L^2 \mu}} \sin\left(\frac{\pi n}{2}\right) \quad (25)$$

$$= \frac{1}{2L} \sum_{n=-N/2}^{+N/2} e^{-\frac{i \pi^2 t n^2}{2L^2 \mu} - \frac{i \pi^2 t n}{2L^2 \mu} + \frac{i \pi x n}{L} - \frac{i \pi^2 t}{8L^2 \mu} + \frac{i \pi x}{2L}} \quad (26)$$

For $N \gg 1$ we can approximate this sum with an integral and thus obtain which reads

$$G^{(0)}(0, 0; x, t) = \frac{1}{2} \sqrt{\frac{\mu}{2\pi i t}} e^{i \frac{\mu x^2}{2t}} \left[\text{Erf}\left(\frac{(\frac{1}{4} + \frac{i}{4})((N+1)\pi t - 2L\mu x)}{L\sqrt{\mu t}}\right) + \text{Erf}\left(\frac{(\frac{1}{4} + \frac{i}{4})((N-1)\pi t + 2L\mu x)}{L\sqrt{\mu t}}\right) \right] \quad (27)$$

In the limit $N \rightarrow \infty$ we can approximate the error functions to one and therefore obtain the exact expression (24).

To further test this formula we can also use the Feynman-Kac formula to extract the ground state energy

$$E_0 = -\lim_{\tau \rightarrow \infty} \frac{1}{\tau} \log \int dx G(x, -i\tau, x, 0). \quad (28)$$

In our case the integral appearing in (28) becomes a sum over all the grid points and therefore reads

$$E_0 = -\lim_{\tau \rightarrow \infty} \frac{1}{\tau} \log \left\{ \frac{1}{Nh} \sum_{k=-N/2+1}^{N/2-1} \sum_{n=-N}^{+N} (i)^{n+1} \sin\left(\frac{n\pi}{2} + \frac{kn\pi}{N}\right) e^{-\tau \left[\frac{1}{2\mu} \left(\frac{n\pi}{2L}\right)^2\right]} e^{i \frac{kn\pi}{N}} \right\}. \quad (29)$$

Because we are taking the limit $\tau \rightarrow \infty$, the exponential factor in this expression will be quite small unless $n = \pm 1$ (the term $n = 0$ vanishes). For this reason we can approximate

$$\begin{aligned} E_0 &= -\lim_{\tau \rightarrow \infty} \frac{1}{\tau} \log \left\{ \frac{1}{Nh} \sum_{k=-N/2+1}^{N/2-1} \left[2e^{-\frac{\pi^2 \tau}{8\mu L^2}} \cos^2\left(\frac{k\pi}{N}\right) \right] \right\} \\ &= -\lim_{\tau \rightarrow \infty} \frac{1}{\tau} \log \left\{ e^{-\frac{\pi^2 \tau}{8\mu L^2}} \right\} = \frac{\pi^2}{8\mu L^2} \end{aligned} \quad (30)$$

which is indeed the exact ground state of the particle in the box.

We can now consider the more general case in which the Hamiltonian contains a potential. In this case the formula of Section IV cannot be applied directly because \hat{p} and \hat{x} do not commute. However we can use the Trotter product formula to write [19, 20]

$$G(y, 0; x, t) = \lim_{N \rightarrow \infty} \langle x | \left(e^{-i \frac{\hat{p}^2}{2\mu N} t} e^{-i \frac{V}{N} t} \right)^N | y \rangle. \quad (31)$$

We can use the completeness of the coordinate states, $|x\rangle$, to write

$$G(y, 0; x, t) = \lim_{N \rightarrow \infty} \sum_{r_1, r_2, \dots, r_N} \langle x | \left(e^{-i \frac{\hat{p}^2}{2\mu N} t} e^{-i \frac{V}{N} t} \right) | x_{r_1} \rangle \langle x_{r_1} | \left(e^{-i \frac{\hat{p}^2}{2\mu N} t} e^{-i \frac{V}{N} t} \right) | x_{r_2} \rangle \dots \langle x_{r_N} | \left(e^{-i \frac{\hat{p}^2}{2\mu N} t} e^{-i \frac{V}{N} t} \right) | y \rangle \quad (32)$$

where the indices r_i span all the lattice. Notice the factors t/\overline{N} , which correspond to having a “time-slicing”, as usual in path integration; at each intermediate time each point on the grid can be reached.

We define

$$\mathcal{V}_N(x_i, t) \equiv h \langle x_i | e^{-i \frac{V(x)}{N} t} | x_j \rangle = e^{-i \frac{V(x_i)}{N} t} \delta_{ij}, \quad (33)$$

which is diagonal in the coordinates. We can now write the compact expression

$$G(y, 0; x, t) = \lim_{\bar{N} \rightarrow \infty} \frac{1}{h^{\bar{N}}} \sum_{r_1, r_2, \dots, r_{\bar{N}}} G^{(0)}(x_{r_1}, t - \varepsilon; x, t) \mathcal{V}_{\bar{N}}(x_{r_1}, t) G^{(0)}(x_{r_2}, t - 2\varepsilon; x_{r_1}, t - \varepsilon) \mathcal{V}_{\bar{N}}(x_{r_2}, t) \dots \mathcal{V}_{\bar{N}}(x_{r_{\bar{N}}}, t) G^{(0)}(y, 0; x_{r_{\bar{N}}}, \varepsilon), \quad (34)$$

where $\varepsilon \equiv t/\bar{N}$. This expression should be compared with the standard path integral expression[19, 20]

$$G(x, t; y, 0) = \lim_{N \rightarrow \infty} \int dx_1 \dots dx_{N-1} \left(\frac{\mu}{2\pi i \epsilon} \right)^{N/2} e^{i\epsilon \sum_{j=0}^{N-1} \left[\frac{\mu}{2} \left(\frac{x_{j+1} - x_j}{\epsilon} \right)^2 - V(x_j) \right]}, \quad (35)$$

where $\epsilon \equiv t/N$.

Our result of eq. (34) provides a new representation of the path integral for quantum mechanical problems with a clear physical interpretation: the propagation of a particle sitting at y at time $t = 0$ and reaching x at time t occurs moving at each time interval, ε , from a point of the grid to another one in all possible ways (remember the sums over the grid points). $G^{(0)}(x_i, t; x_j, t + \varepsilon)$ represents the probability of going from a point x_i to another point x_j on the grid in a time interval ε ; at this point an interaction take place, through the the potential term \mathcal{V} . We stress that our representation corresponds to a different way of discretizing space which also allows to deal with Hamiltonians containing non-local operators (the SSE is one example) and could be an useful tool for problems which cannot be easily treated with the conventional formalism.

V. CONCLUSIONS

In this paper we have derived an analytical expression for the non-local relativistic kinetic energy operator which appears in the Salpeter equation. This representation is exact in the limit of an arbitrarily fine grid and we have used it to solve the Salpeter equation for the Relativistic Harmonic Oscillator, where semi-analytical results are available. We have found that our representation can be used together with the Variational Sinc Collocation Method (VSCM) to provide arbitrarily precise results, with a strong rate of convergence. The most important result of this paper is the new representation for the quantum mechanical Green's function, which requires the evaluation of matrix elements of non-local operators. We have provided a general formula and we have explicitly tested it in the case of a free particle in a box, recovering the exact result. Our new representation of the path integral can be applied also to problems in which the Hamiltonian contains non-local operators (which would be the case of the Salpeter equation) and it is suitable both for numerical and analytical calculations, in the cases in which the limits $N, \bar{N} \rightarrow \infty$ can be calculated (as for a free particle in a box).

Given the importance of path integrals in many areas of Physics, we feel that the results contained in this paper could have a large number of applications. Finally, we wish to mention that it would be worth exploring the possibility to use the PMS in a numerical scheme to optimize convergence to the exact result for finite values of N and \bar{N} . It also remains to explore the possibility to apply our formalism to Quantum Field Theory (QFT), which we plan to address in future works.

-
- [1] L.J.Nickisch, L.Durand and B.Durand, Phys. Rev. D **30**, 660 (1984)
 - [2] C. Long, Phys. Rev. D **30**, 1970 (1984)
 - [3] W. Lucha, H. Rupprecht and F. Schöberl, Phys. Rev. D **45**, 1233-1239 (1992)
 - [4] L.P. Fulcher, Phys. Rev. D **50**, 447 (1994)
 - [5] J.W. Norbury, K. Maung Maung and D. E. Kahana, Phys. Rev. D **50**, 3609 (1994)
 - [6] P. Amore, A variational sinc collocation method for strong coupling problems, Journal of Physics **A** 39, L349-L355 (2006)
 - [7] P. Amore, M. Cervantes and F.M. Fernández, ArXiv:[quant-ph/0608069] (2006)
 - [8] W. Lucha and F. Schöberl, Phys. Rev. A **54**, 3790-3794 (1996)
 - [9] W. Lucha and F.F. Schöberl, J. Math. Phys. **41**, 1778 (2000)
 - [10] R. Hall, W. Lucha and F. Schöberl, J. Phys. A **34**, 5059-5063 (2001)
 - [11] R. Hall and W. Lucha, J. Phys. A **38**, 7977-8002 (2005)
 - [12] W. Lucha and F.F. Schöberl, Phys. Rev. A **51**, 4419- 4426 (1995)
 - [13] C. Semay, D. Baye, M. Hesse and B. Silvestre-Brac, Phys. Rev.E **64**, 016703 (2005)
 - [14] L. Zhi-Feng, L. Jin-Jin, W. Lucha, M. Wen-Gan and F. Schöberl, J. Math. Phys. **46**, 103514 (2005)
 - [15] P. Amore, A. Aranda, F.M. Fernández and H.F. Jones, Physics Letters A **340**, 87-93 (2005)

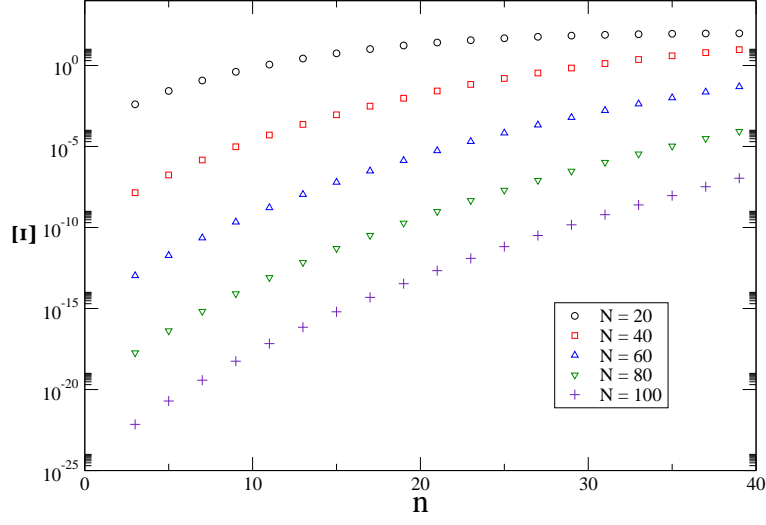


FIG. 1: Error for the coefficient $\bar{\epsilon}_n$ (in %) (color online).

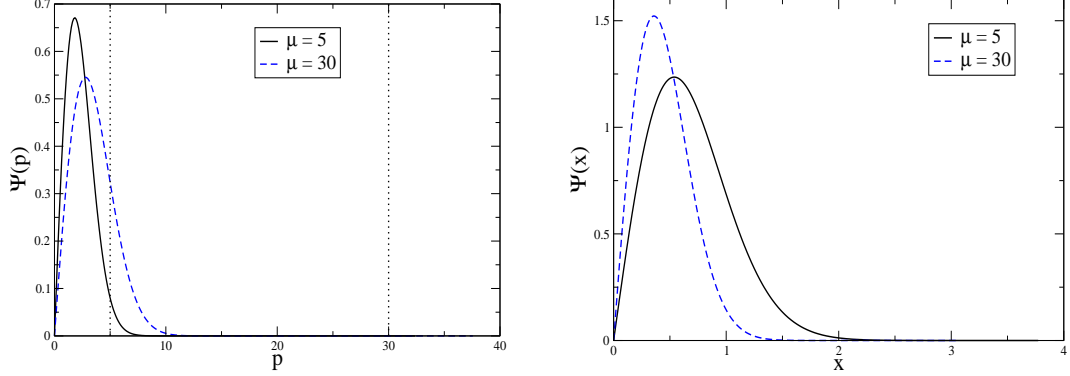


FIG. 2: Left Plot: Wave functions in momentum space for the RHO with $\mu = 5$ (solid line) and $\mu = 30$ (dashed line). The vertical lines correspond to the two values of μ . Right Plot: Wave functions in coordinate space for the RHO with $\mu = 5$ (solid line) and $\mu = 30$ (dashed line). We have used $N = 50$ (color online).

- [16] P. M. Stevenson, Phys. Rev. D **23**, 2916 (1981).
- [17] A. Kempf, G. Mangano and R.B. Mann, Phys. Rev. D **52** 1108 (1995)
- [18] R. Easther, G. Guralnik and S. Hahn, Phys. Rev. D **61**, 125001 (2000)
- [19] R.P. Feynman and A.R. Hibbs, Quantum mechanics and path integrals, McGraw-Hill, New York (1965)
- [20] L.S. Schulman, Techniques and applications of Path Integration, John Wiley and Sons, New York (1981)

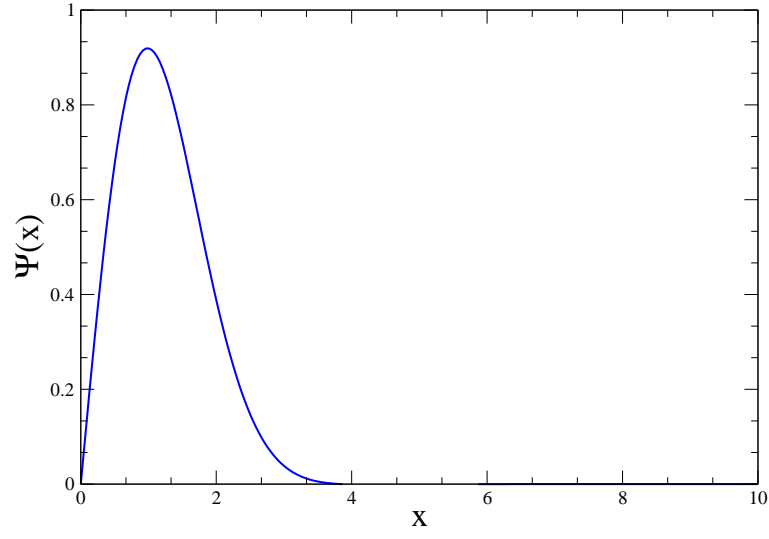


FIG. 3: Wave function for the ground state of the SSE of eq. (20) with $\mu = a = 1$ in coordinate space. We have used $N = 100$ (color online).